

## **Electronic Supplementary material**

### **Exploring the intrinsic behaviour of multi-site phosphorylation systems as part of signalling pathways.**

Thapanar Suwanmajo <sup>1,2,3</sup> and J. Krishnan <sup>1,4\*</sup>

<sup>1</sup> Centre for Process Systems Engineering, Department of Chemical Engineering, Imperial College London, London SW7 2AZ, UK

<sup>2</sup> Center of Excellence in Materials Science and Technology, Chiang Mai University, Chiang Mai 50200, Thailand.

<sup>3</sup> Department of Chemistry, Faculty of Science, Chiang Mai University, Chiang Mai 50200, Thailand.

<sup>4</sup> Institute for Systems and Synthetic Biology, Imperial College London, South Kensington Campus, London SW7 2AZ, UK.

\*j.krishnan@imperial.ac.uk. Ph: 44-20-7594-6633; Fax: 44-20-7594-6606.

In this supplementary material, we present a number of details related to the material presented in the main text: (i) information regarding parameters used in the main text in the figures and (ii) additional figures, which complement those in the main text (and in some cases referred to there).

#### **1 Comments on parameters**

Before presenting the parameters, we make a number of comments about parameters in the context of our results. At the outset we note that multisite modification is intrinsically capable of displaying different kinds of qualitative behaviour and this depends on the parameter regime. This has been studied in the literature both computationally and analytically. While there are multiple parameters (binding, unbinding and catalytic constants as well as total amounts of

substrate and enzyme) which can affect the behavior of the systems, the catalytic constants are particularly important (especially the variation across cycles) to enable certain behavior such as bistability. As a reference (Conradi and Mincheva, 2014) have characterized a single inequality involving the four catalytic constants as an enabler of bistability. With this being satisfied, enzyme and substrate amounts can be varied to realize bistability. On the other hand guaranteeing a single steady state depends on two inequalities being satisfied, one involving catalytic constants and the other involving catalytic constants and  $K_m$  values. Clearly there are broad ranges of parameter space (intrinsic kinetic constants) which satisfy each of these conditions. Similarly, it is possible to choose parameter regions which allow for biphasic responses in the maximally modified phosphoform, and this origins of this behavior are studied in (Suwanmajo and Krishnan, 2013). Finally monostable switch like behavior can also be obtained, and this has been studied in the literature. This can be obtained even with (de)phosphorylation catalytic constants the same across cycles. This provides useful input to our study.

Noting the multiple types of qualitative behavior intrinsically possible, we recognize at the outset that enzyme activation/downstream coupling can have multiple qualitative effects: (i) A transition to a different type of behaviour seen in the multisite modification system (ii) No transition (iii) A transition to new behaviour which cannot be seen (or has not been reported) in the multisite module in isolation. This frames our approach to parameters and analysis.

Our focus is on non-trivial qualitative effects and (sets of) transitions in behavior introduced by either the enzyme activation step or by downstream coupling. At the outset, we note that the results presented in the paper are underpinned by broad range of computational investigations. Based on this broad range, we identified different sets of non-trivial transitions which emerge: this includes transitions which are seen repeatedly (in multiple different parameter regions and in fact even in different model variants), along with some notable new behavior. The text presents both kinds of results, computationally, complementing them with analytical results. We detail this further below.

- (i) The results in the main text involved a combination of computational demonstrations, of various behavior and transitions introduced by enzyme activation or downstream

- coupling. This was complemented by analytical results in multiple specific regimes to rule out transitions.
- (ii) In all the computational results, parameters for both the intrinsic kinetics of multisite modification as well the enzyme activation or downstream modules were chosen as discussed below.
  - (iii) With regard to the parameters for enzyme activation, there are basically two additional parameters for each enzyme (activation/inactivation). These rates are chosen not to be high relative to the intrinsic kinetics of multisite modification. Furthermore the ratio allows a “healthy” balance between active and inactive form, so that no form dominates (unless as mentioned in a specific instance, we ensure the enzyme is active).
  - (iv) With regard to downstream coupling, we primarily work with two sets of parameters for the downstream covalent modification cycle kinetics. The difference is in the phosphorylation step which affects the extent of (upstream) substrate sequestration.
  - (v) For the multisite modification module, we choose different parameter sets representative of different regimes (e.g. bistability, monostable switch etc). These are of course not unique, but have been characterized (in some cases broadly) in the literature, as discussed above. In most of these cases, we have seen similar computational trends (i.e class of transition) or results in another parameter regime representing the same behavior. This indicates that there is nothing special about the basal parameter regime (see below). We discuss this further below. Occasionally there may be special behavior observed and reported (and noted as such in the main text), but even this is seen in a range of parameters.
  - (vi) At the outset, we note that the computational results fall into different categories (a) Results representative of broad trends (b) Results directly demonstrating a particular (non-trivial) behavior and transition (c) Results making controlled comparisons to demonstrate specific points. (a) and (b) constitute most of the computational results.
  - (vii) Enzyme activation: (Figs. 2-5) The fact that oscillations emerge is seen in multiple regimes starting from both monostable and bistable regimes of the intrinsic kinetics (and in different variants of multisite models) oscillations can result. Of course, they are not guaranteed to result (for instance if all steps of the multisite module are in an

unsaturated regime as we have already noted), but this is seen in broad regimes. Thus this represent a representative class of transitions. The fact that bistable dose-response curves can be switched to monostable dose response curves and vice versa, is also suggested by analysis (and noting the behavior of a multisite module in isolation to changes in its parameters). The fact that random mechanisms with kinetic symmetry can realize oscillations (with enzyme activation) is a consolidation of this. Complex oscillations, on the other hand are not routinely observed, and emerged after a broad computational investigation. This is an example of a computational result directly demonstrating the presence of some non-trivial and unexpected behavior.

- (viii) Downstream coupling: (Fig 6): Some of the results, such as diminishing of amplitude of monostable switch, and diminishing of biphasic responses are seen very broadly and are representative. The creation of bistability and oscillations is seen with sufficient sequestration. We have already noted that depending on the rate constants associated with phosphorylation downstream, the same module in isolation gave either bistability and bistability with oscillations. In any case both these results are demonstrations of non-trivial behavior which can emerge. (Fig. 7): This directly shows how bistability can be perturbed in different ways. One is to a monostable curve, which is seen broadly and is in some sense an expected kind of transition. However bistability can also be perturbed differently, giving rise to tristability. This is again a kind of behavior, for which the computation provides a direct demonstration. The downstream dephosphorylation in a saturated regime (Fig. 8): The main point here is how plateau like regions can emerge, which is in fact seen across multiple parameter sets of the basal module. This by itself demonstrates that it is present when other parameters are changed (to the point that the intrinsic behavior of the module is markedly different). Figure S4 demonstrates the similar behavior even with two separate kinases and a common phosphatase. Furthermore the computations here when compared with the case of App sequestration (done for the same sets of multisite and downstream parameters) directly support the conclusion that sequestration of different phosphoforms can be associated with different trends. (Fig. 9): This is a combination of a behavior (enzyme activation resulting in oscillations) broadly seen, and another behavior (sequestration resulting in the destruction of

behavior and resulting in a monostable dose response curve) which is broadly representative. The reverse of the enzyme activation step destroying oscillations which emerge from downstream activation is seen when the activation/inactivation steps are not too fast (relative to the intrinsic kinetics of the modification).

- (ix) Design of multisite modification: (Fig. 10): Varying of kinase activation signal resulting in a range of oscillations, is seen across multiple parameter sets. The case of creation of bistability for a range of signal  $S_1$  (while the high  $S_1$  limit is monostable) and the other way around, is also seen in multiple parameter regimes, This figure simply makes the point that varying the second enzyme activation signal can have different effects, which is directly shown. (Fig. 11). A direct demonstration that a random mechanism with different kinases and phosphatases can give rise to oscillations.

## 2 Parameter values in the Figures

We present here some details regarding the parameters employed in the computational results presented in the main text. The parameters are all dimensionless parameters. The paper analyses the information processing capabilities of multi-site phosphorylation systems in which substrate is in excess over (phosphatase) enzyme. In all the numerical simulation and bifurcation analysis, unless otherwise mentioned, the initial conditions of substrate, also equal to total concentration of substrate ( $A_{tot}$ ), and phosphatase, ( $P_{tot}$ ), are 40 and 1. The initial condition for the substrate corresponds to all substrate being present in the unmodified form. Likewise, the initial condition for the kinase and phosphatase is for all the enzyme to be present in the inactive form if enzyme activation is present, or in the free (active) form, if no activation is present. In any case the concentrations of the various complexes are zero initially. Furthermore, enzyme (de)activation parameters as well as kinetic parameters such as binding, unbinding and catalytic constants are equal to 1, unless otherwise mentioned. In particular the unbinding constants are never changed in our study. All simulation results from phosphorylation models here correspond to models with either upstream or downstream coupling (or both). The schematics for the various models are presented in Figure 1 of the main text. A detailed kinetic reaction depiction illustrated in Figure S6 and S7 (in the supplementary information) and Figure 1 (in the main text).

**Figure 2** Parameters for the ordered, distributive double-site phosphorylation model with explicit activation (model E1)

(a) Isolated system (model M1):  $K_{\text{tot}} = 17$ ,  $P_{\text{tot}} = 17$ ,  $k_7 = 200$  and  $k_{12} = 40$ .

(b, c) Isolated system (model M1): the same parameters as fig 2(a).

Explicit activation model (E1):  $k_{a,P} = 0.032$  and  $k_3 = 0.6$ .

(d) Isolated system (model M1):  $K_{\text{tot}} = 30$ ,  $P_{\text{tot}} = 17$ ,  $k_1 = 10$ ,  $k_7 = 100$ ,  $k_{12} = 40$ .

(e, f) Isolated system (model M1): the same parameters as fig 2(d).

Explicit activation model (E1):  $S_1 = S_2 = 0.5$ ,  $k_{a,P} = 0.32$  and  $k_3 = 0.8$ .

**Figure 3** Parameters for explicit activation models where kinase is shared (model E1) or separated (model E2).

(a) Model E1: the same parameters as figure 2e.

(b) Model E1: the same parameters as figure 2b.

(c) Model E2:  $K_{1,\text{tot}} = K_{2,\text{tot}} = P_{\text{tot}} = 17$ ,  $k_4 = 0.1$ ,  $k_6 = 10$ ,  $k_7 = 200$ ,  $k_{12} = 40$ ,  $k_{a,K1} = k_{a,K2} = 0.5$  and  $k_{a,P} = 0.032$ .

**Figure 4** Parameters for complex oscillations in explicit activation model (model E1)

(a, b)  $S_1 = S_2 = 0.1$ ,  $k_3 = 1$  and other parameters are the same as figure 2(b).

(c)  $K_{\text{tot}} = 30$ ,  $P_{\text{tot}} = 1$ ,  $k_1 = 100$ ,  $k_3 = 0.01$ ,  $k_7 = 100$ ,  $k_9 = 0.9$ ,  $k_{10} = 3$ ,  $k_{12} = 10$ ,  $k_{13} = 0.1$  and  $k_{15} = 0.1$   
 $S_1 = 0.0275$ ,  $S_2 = 0.03$ .

**Figure 5** Parameters for explicit activation models where phosphorylation is ordered (model E1) or random (model M3).

(a) Model E1

Isolated system (model M1):  $K_{\text{tot}} = 23$ ,  $P_{\text{tot}} = 17$ ,  $k_7 = 200$  and  $k_{12} = 40$ .

Explicit activation (Model E1):  $K_{\text{tot}} = 23$ ,  $P_{\text{tot}} = 17$ ,  $k_7 = 200$ ,  $k_{12} = 40$ ,  $k_{i,K} = 0.01$  and  $k_{a,P} = 0.5$ .

(b) Model E1

$$K_{\text{tot}} = 30, P_{\text{tot}} = 17, k_7 = 20.$$

(c) Model M3 with explicit activation

(i) Isolated system (Model M3):  $K_{\text{tot}} = P_{\text{tot}} = 17, k_{13} = k_{18} = k_{19} = k_{24} = 40$ .

(ii) Model M3 with explicit activation:  $K_{\text{tot}} = P_{\text{tot}} = 17, k_{13} = k_{18} = k_{19} = k_{24} = 40$  and  $k_{a,P} = 0.032$ .

**Figure 6** Parameters for ordered, double distributive phosphorylation with downstream coupling: the downstream covalent modification cycle (CMC) is catalysed by the fully modified form (model R1). Here upstream refers to the multisite substrate modification (model M1).

(a) Upstream module:  $A_{\text{tot}} = 10, P_{\text{tot}} = 0.1$  and  $k_1 = 0.1$

Downstream CMC:  $k_{13} = 100, k_{16} = 100, F_{\text{tot}} = 7$

$X_{\text{tot}}$  were varied, taking values 0, 5, 10 and 15.

(b) Upstream module:  $A_{\text{tot}} = 35, P_{\text{tot}} = 2$  and  $k_6 = 0.01$ .

Downstream CMC:  $k_{13} = 100, k_{15} = 0.1, k_{16} = 200, F_{\text{tot}} = 2$

$X_{\text{tot}}$  were varied, taking values 0, 3, 6 and 9.

(c, d, e) Upstream module:  $A_{\text{tot}} = 10, P_{\text{tot}} = 0.1, k_1 = k_4 = 100, k_3 = k_6 = 0.1$  and  $k_7 = 50$

Downstream CMC:  $k_{13} = 100, k_{16} = 100, F_{\text{tot}} = 7$  and  $X_{\text{tot}} = 150$ .

(f, g, h) Upstream module: the same parameters as figure 6(c).

Downstream CMC:  $k_{13} = 10, k_{15} = 0.1$  and  $k_{16} = 100, F_{\text{tot}} = 7$

$X_{\text{tot}}$  were varied, taking values 10, 20 and 30.

**Figure 7** Parameters for ordered, double distributive phosphorylation with downstream coupling (model R1).

(a, b, c) Upstream module:  $A_{\text{tot}} = 10, P_{\text{tot}} = 0.1, k_1 = k_4 = 100, k_3 = 0.1, k_6 = 10$  and  $k_7 = 50$ .

Downstream CMC:  $k_{13} = 100, k_{16} = 100, F_{\text{tot}} = 7$ .

$X_{\text{tot}}$  were varied, taking values 0, 10, 20 and 30.

(d, e) Upstream module:  $A_{\text{tot}} = 10$ ,  $P_{\text{tot}} = 1$ ,  $k_1 = 100$  and  $k_3 = 0.4$ .

Downstream CMC:  $X_{\text{tot}} = 100$  and other parameters are the same parameters as figure 7(b).

**Figure 8** Parameters for ordered, double distributive phosphorylation with downstream coupling: the downstream covalent modification cycle (CMC) is catalysed by partially modified form (model R2).

(a,b) Upstream module: the same parameters as figure 6(c).

Downstream CMC: the same parameters as figure 6(d).

$X_{\text{tot}}$  were varied, taking values 0, 30, 60 and 90.

(c,d) Upstream module: the same parameters as figure 6(b)

Downstream CMC: the same parameters as figure 6(b)

$X_{\text{tot}}$  were varied, taking values 0, 10, 20, 30 and 40.

(e,f) Upstream module: the same parameters as figure 7(a).

Downstream CMC: the same parameters as figure 7(b).

$X_{\text{tot}}$  were varied, taking values 0, 30, 60 and 90.

**Figure 9** Parameters for the interplay of upstream and downstream coupling, model R1 with explicit activation (E1).

(a) Explicit activation (model E1):  $K_{\text{tot}} = 28$ ,  $P_{\text{tot}} = 17$ ,  $k_3 = 0.6$ ,  $k_7 = 100$ ,  $k_{12} = 40$  and  $k_{a,P} = 0.2$ .

(b) Explicit activation: the same parameters as figure 9(a).

Model R1:  $k_{13} = 100$ ,  $k_{15} = 0.5$ ,  $k_{18} = 0.1$  and  $F = 7$

$X_{\text{tot}}$  were varied, taking values 30, 60 and 90.

(c) Model R1: the same parameters as figure 6(d).



(d) Model R1: the same parameters as figure 6(d).

. Explicit activation (model E1):  $K_{a,P} = 15$ .

$K_{a,K}$  were varied, taking values 0.5, 0.05 and 0.01.

**Figure 10** Parameters for model E1.

(a)  $K_{tot} = P_{tot} = 17$ ,  $k_1 = 200$ ,  $k_3 = 2$ ,  $k_7 = 200$ ,  $k_9 = 0.3$ ,  $k_{10} = 2$  and  $k_{12} = 40$ .

$S_2$  were varied, taking values 0.05, 0.07 and 0.5.

(b)  $K_{tot} = P_{tot} = 17$ ,  $k_1 = 200$ ,  $k_6 = 40$ .

.  $X_{tot}$  were varied, taking values 1, 10 and 100.

(c)  $K_{tot} = P_{tot} = 17$ ,  $k_1 = 200$ ,  $k_7 = 200$ ,  $k_9 = 0.3$ ,  $k_{10} = 2$  and  $k_{12} = 40$ .

.  $S_2$  were varied, taking values 0.32, 1 and 10.

**Figure 11** Parameters for isolated systems of random, distributive double-site phosphorylation model through separate kinases and separate phosphatases (model M4)

g(i-ii)  $K_{1,tot} = K_{2,tot} = 9$ ,  $k_{13} = 10$ ,  $k_{14} = k_{15} = k_{17} = k_{18} = 0.1$ ,  $k_{19} = k_{22} = 80$ ,  $k_{21} = 0.9$ ,  $k_{24} = 30$ ,  $P_{1,tot} = 8$  and  $P_{2,tot} = 6$

g(iii)  $P_{1,tot} = P_{2,tot} = 0.5$ ,  $k_1 = k_4 = k_7 = k_{10} = k_{13} = k_{16} = k_{19} = k_{22} = 10$ ,  $k_3 = k_9 = 0.1$  and  $K_{1,tot} = K_{2,tot} = 1$

## Supplementary figure:

**Figure S1** Parameters for model M1 (or model M2) in which phosphatase is shared with single site covalent modification.

(a)

Model M1:  $K_{\text{tot}} = 21$ ,  $P_{\text{tot}} = 24$ ,  $k_1 = 9$ ,  $k_3 = 2.9$ ,  $k_7 = 200$ ,  $k_8 = 0.1$ ,  $k_{10} = 30$ ,  $k_{12} = 40$ .

Single covalent modification:  $X_{\text{tot}} = 24$ ,  $E_{\text{tot}} = 17$ ,  $k_{15} = 10$ ,  $k_{16} = 0.24$ ,  $k_{17} = 0.012$  and  $k_{18} = 0.001$ .

(b)

Model M2:  $A_{\text{tot}} = 40$ ,  $K_{1,\text{tot}} = K_{2,\text{tot}} = 17.1$ ,  $P_{\text{tot}} = 24$ ,  $k_1 = 9$ ,  $k_3 = 2.9$ ,  $k_5 = k_6 = 0.5$ ,  $k_7 = 200$ ,  $k_8 = 0.1$ ,  $k_{10} = 30$ ,  $k_{12} = 4$ .

Single covalent modification:  $X_{\text{tot}} = 17$ ,  $E_{\text{tot}} = 17$ ,  $k_{15} = 10$ ,  $k_{16} = 0.24$ ,  $k_{17} = 0.012$  and  $k_{18} = 0.001$ .

**Figure S2** Parameters for model R3: the downstream covalent modification cycle (CMC) is catalysed by both fully and partially modified form. Here upstream refers to the multisite substrate modification (model M1).

Upstream module: parameters are the same as figure 6(c).

Covalent modification cycle of X:  $k_{13} = 10$ ,  $k_{15} = 0.1$ ,  $k_{16} = 100$ .  $F_{1,\text{tot}} = 7$ .

Covalent modification cycle of Y:  $k_{19} = 10$ ,  $k_{21} = 0.1$ ,  $k_{22} = 100$ .  $F_{2,\text{tot}} = 7$ .

(a)  $X_{\text{tot}} = Y_{\text{tot}} = 0$ , (b)  $X_{\text{tot}} = 10$ ,  $Y_{\text{tot}} = 0$ , (c)  $X_{\text{tot}} = 0$ ,  $Y_{\text{tot}} = 10$ , (d)  $X_{\text{tot}} = 10$ ,  $Y_{\text{tot}} = 10$ .

(e)  $X_{\text{tot}} = 20$ ,  $Y_{\text{tot}} = 0$ , (f)  $X_{\text{tot}} = 0$ ,  $Y_{\text{tot}} = 20$ , (g)  $X_{\text{tot}} = 20$ ,  $Y_{\text{tot}} = 20$ .

(h)  $X_{\text{tot}} = 30$ ,  $Y_{\text{tot}} = 0$ , (i)  $X_{\text{tot}} = 0$ ,  $Y_{\text{tot}} = 30$ , (j)  $X_{\text{tot}} = 30$ ,  $Y_{\text{tot}} = 30$ .

**Figure S3** Parameters for model R4: the downstream covalent modification cycle (CMC) is catalysed by fully modified form. Here upstream refers to the multi-site substrate modification through separate kinases and share phosphatase (model M2).

(a) Upstream module:  $k_1 = 2$ ,  $k_{10} = 100$ ,  $P_{\text{tot}} = 0.5$ ,  $A_{\text{tot}} = 10$  and  $K_{2,\text{tot}} = 0.5$ .

Covalent modification cycle:  $k_{13} = 10$ ,  $k_{15} = 0.1$ ,  $k_{16} = 10$  and  $F_{1,\text{tot}} = 1$ .

$X_{\text{tot}}$  were varied, taking values 0, 5, 10 and 15.

(b) Upstream module:  $k_1 = 2$ ,  $k_7 = 100$ ,  $P_{\text{tot}} = 0.3$  and  $K_{2,\text{tot}} = 0.5$ .

Covalent modification cycle:  $k_{13} = 10$ ,  $k_{15} = 0.1$ ,  $k_{16} = 10$  and  $F_{1,\text{tot}} = 1$ .

(ii)  $X_{\text{tot}} = 5$ , (iii)  $X_{\text{tot}} = 10$  and (iv)  $X_{\text{tot}} = 15$ .

**Figure S4** Parameters for model R5: the downstream covalent modification cycle (CMC) is catalysed by partially modified form. Here upstream refers to the multisite substrate modification with separate kinases and share phosphatase (model M2).

(a) Model R5

(i) Upstream module (model M2):  $k_1 = k_4 = 100$ ,  $k_3 = k_6 = 0.1$ ,  $k_7 = 50$ ,  $P_{\text{tot}} = 0.1$ ,  $A_{\text{tot}} = 10$ ,  $K_{1,\text{tot}} = 1$ .

(ii) Covalent modification cycle:  $k_{13} = 100$ ,  $k_{16} = 100$  and  $F_{1,\text{tot}} = 7$ .

$X_{\text{tot}}$  were varied, taking values 0, 30, 60 and 90

(b) Model R5

(i) Upstream module (model M2):  $k_1 = k_4 = 100$ ,  $k_3 = k_6 = 0.1$ ,  $k_7 = 50$ ,  $P_{\text{tot}} = 0.1$ ,  $A_{\text{tot}} = 10$ ,  $K_{2,\text{tot}} = 0.7$ .

(ii) Covalent modification cycle:  $k_{13} = 100$ ,  $k_{16} = 100$  and  $F_{1,\text{tot}} = 7$ .

$X_{\text{tot}}$  were varied, taking values 0, 5, 10 and 15.

**Figure S5** Parameters for model M1 with downstream coupling: open system of single site covalent modification.

Upstream module (model M1):  $k_1 = k_4 = 100$ ,  $k_3 = k_6 = 0.1$ ,  $k_7 = 200$ ,  $k_{10} = 0.5$  and  $k_{12} = 200$ .

Covalent modification cycle (open system):  $k_{13} = 100$ ,  $k_{16} = 100$ ,  $F_{\text{tot}} = 7$ ,  $k_0 = 0.01$  and  $k_d = 0.1$ .

**Note:** ODE equations for  $[X]$ ,  $[X^*]$ ,  $[XA_{\text{pp}}]$  and  $[X^*F]$  become:

$$d[X]/dt = k_0 + k_{14}[A_{\text{pp}}X] - k_{13}[A_{\text{pp}}][X] + k_{18}[X^*F]$$

$$d[A_{\text{pp}}X]/dt = k_{13}[A_{\text{pp}}][X] - (k_{14} + k_{15})[A_{\text{pp}}X]$$

$$d[X^*]/dt = k_{15}[A_{\text{pp}}X] + k_{17}[X^*F] - k_{16}[X^*][F] - k_d[X^*]$$

$$d[X^*F]/dt = k_{16}[X^*][F] - (k_{17} + k_{18})[X^*F]$$

**Figure S8** Parameters for model R1. Here upstream refers to the multisite substrate modification (model M1).

Upstream module (model M1): the same parameters as figure 7(a)

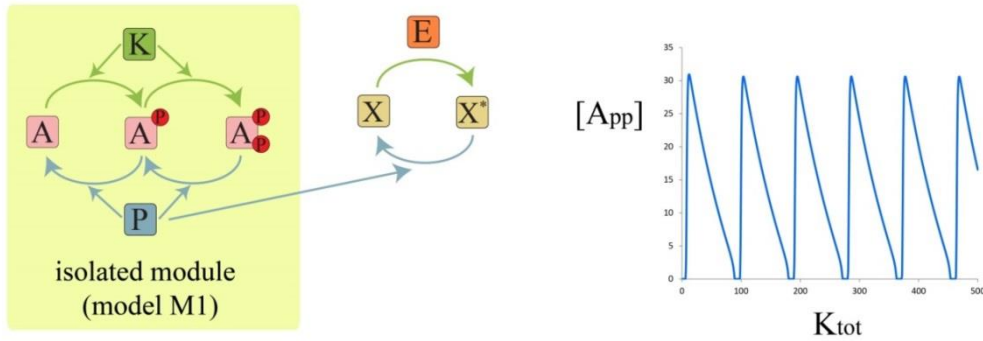
Covalent modification cycle (open system): the same parameters as figure 7(b)

(a)  $X_{\text{tot}} = 130$

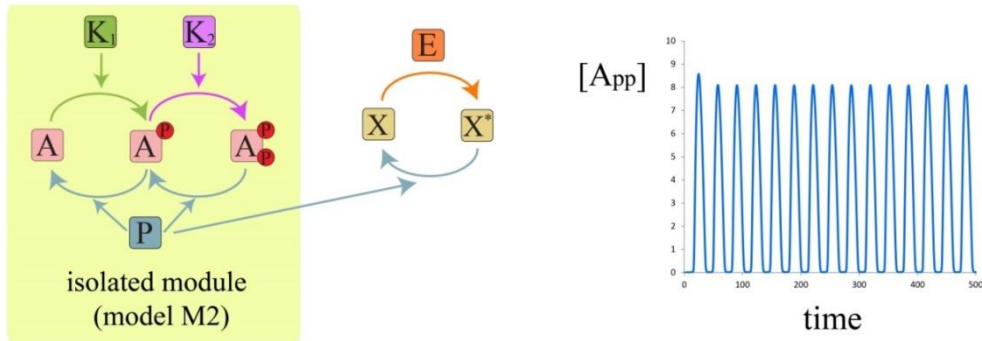
(b)  $X_{\text{tot}} = 200$

## 2 Additional figures

(a)



(b)



(c) Single-site covalent modification cycle in which demodifying enzyme (phosphatase) is shared between this system and Model M1 (or Model M2)

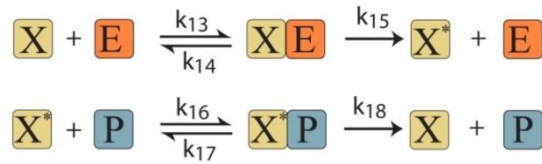


**Figure S1 One shared enzyme between an ordered, double distributive phosphorylation and single covalent modification is sufficient to generate sustained oscillations** (a) De-modifying enzyme (phosphatase) shared between the distributive double-site modification (model E1) and single-site covalent modification can induce sustained oscillations. (b) Sharing phosphatase between double-site modification with separate kinases (model E2) and a single-site covalent modification is also capable of generating sustained oscillation. (c) A depiction of the single-site covalent modification model, where the phosphatase is shared.

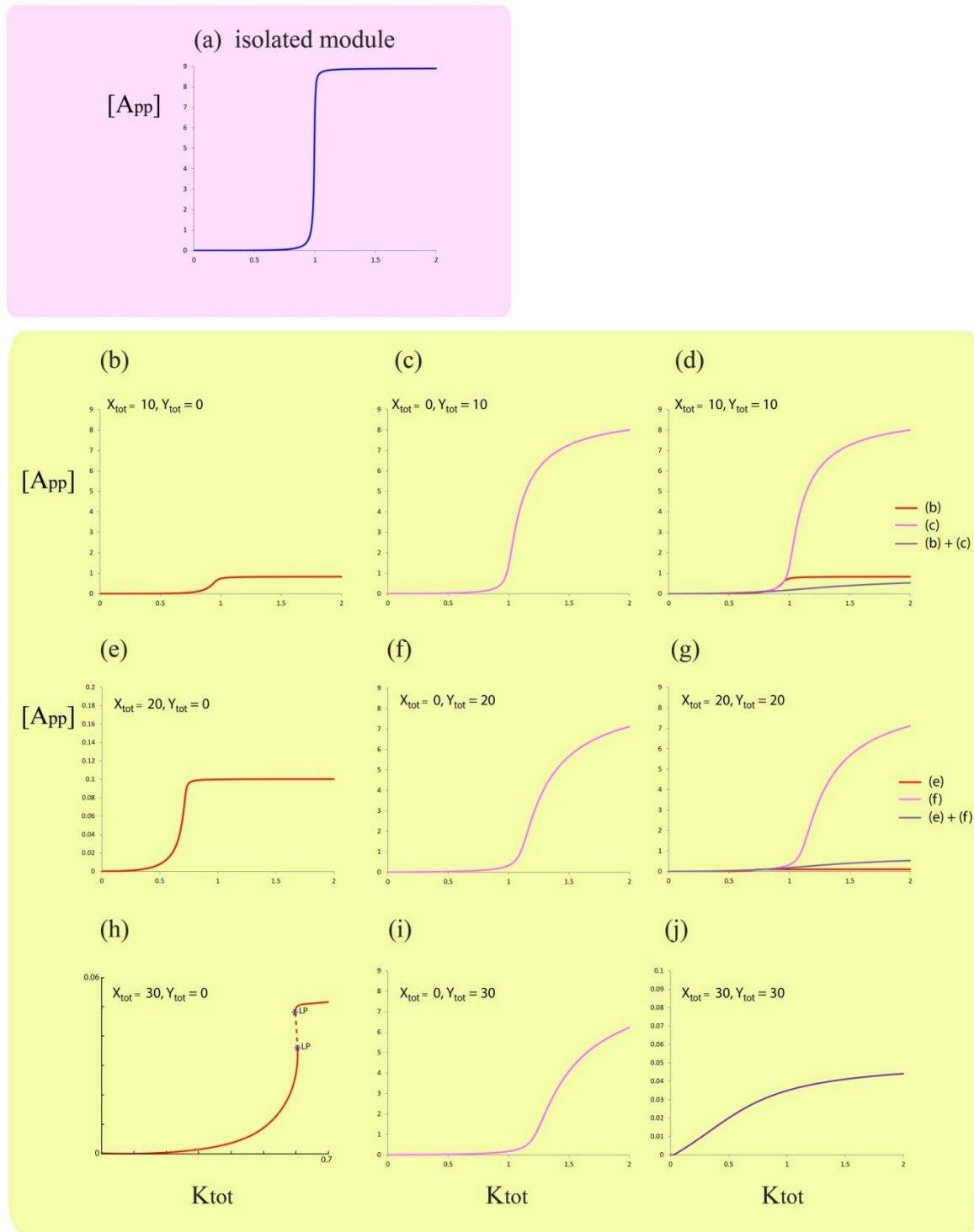


**Figure S2 The effect of sequestration of both phosphoforms in different downstream pathways (denoted by X and Y). A sample demonstration of dose-response curves of  $A_{pp}$  as a function of  $K_{tot}$ : (a) isolated system. (b-j) systems with downstream coupling (model R3).**

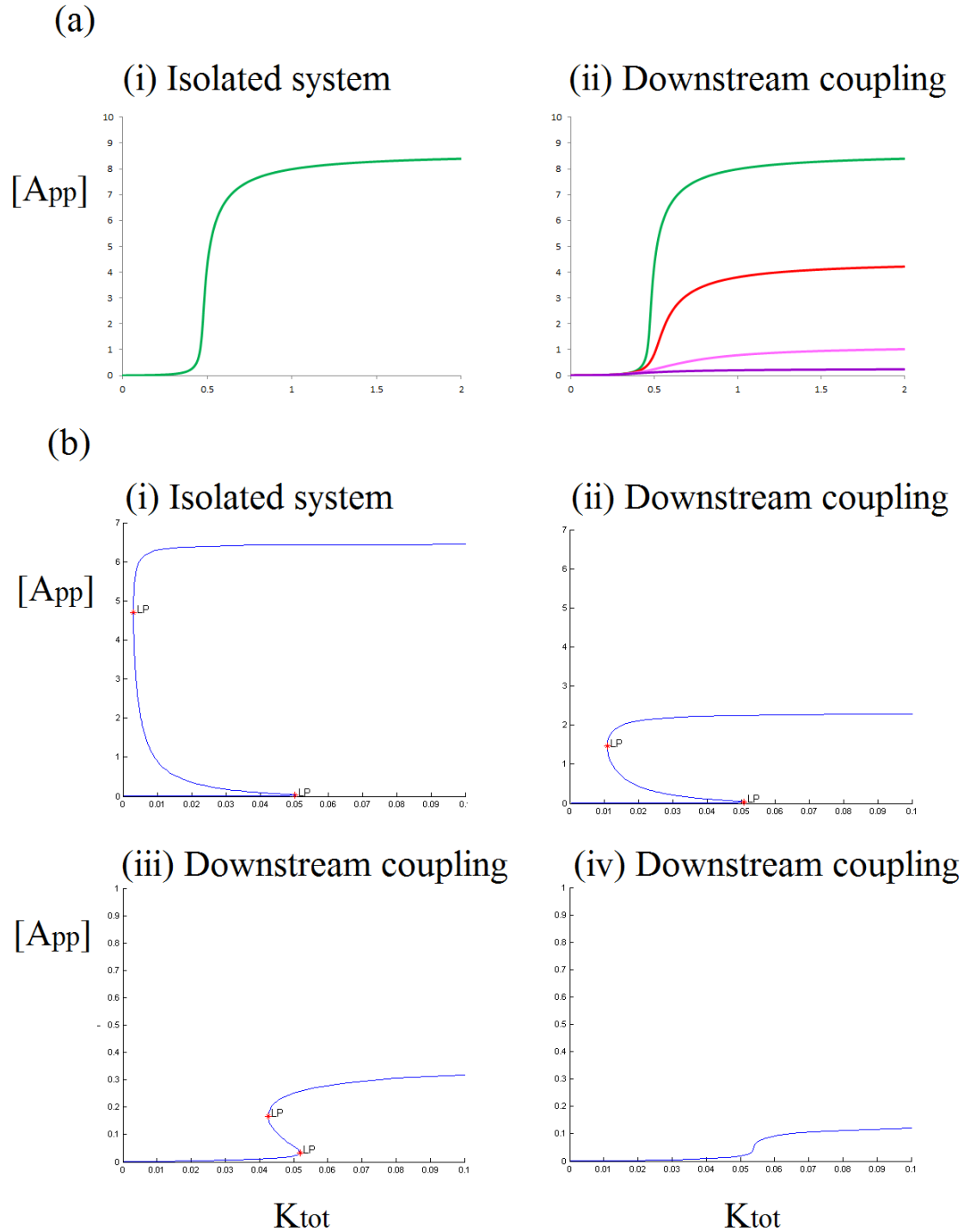
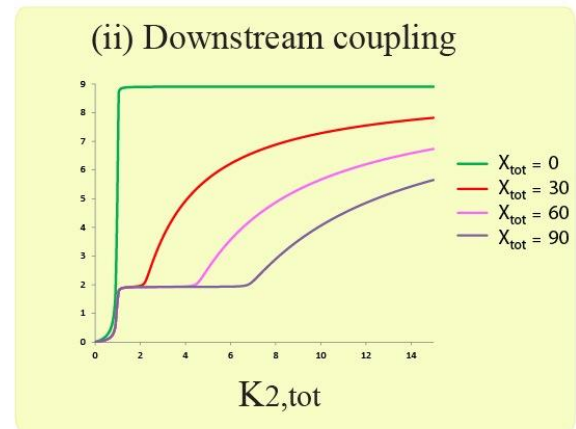
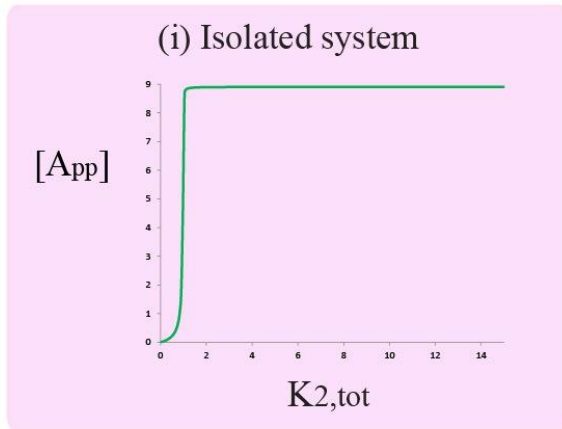


**Figure S3** Effect of  $A_{pp}$  sequestration downstream for the case of multisite modification with separate kinases and a common phosphatase (model R4). (a) shows how downstream coupling quantitatively distorts the response in the case where the double-site module exhibits a sigmoidal dose response. (b) shows how bistability is eventually destroyed.

(a)



(b)

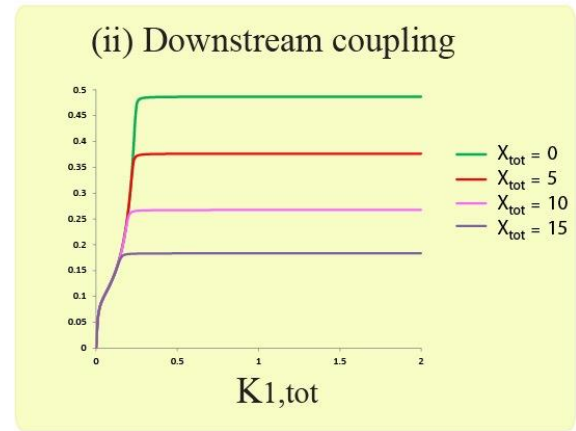
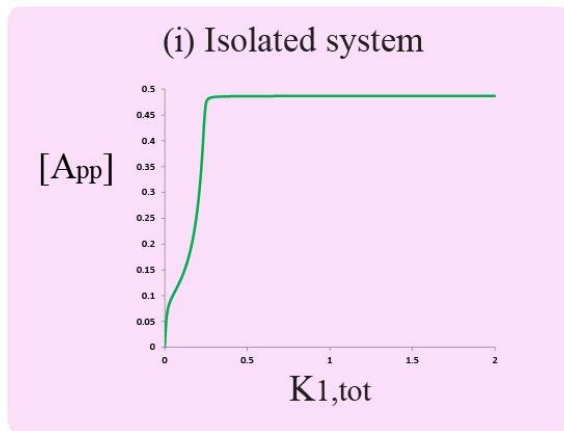
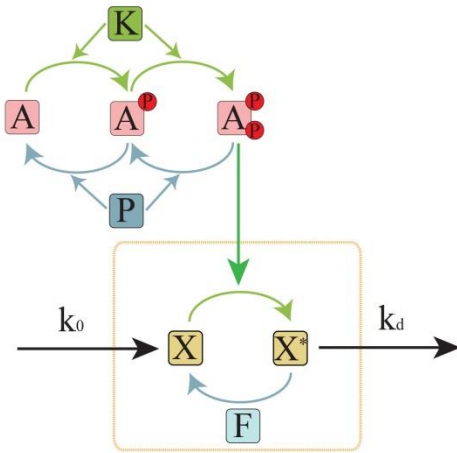


**Figure S4** Effect of  $A_p$  sequestration downstream for the case of multisite modification with separate kinases and a common phosphatase (model R5). Note that the plateau-like behavior emerges when the second kinase concentration is varied. This consolidates our understanding in the main text.

(a) Model R6



(b)

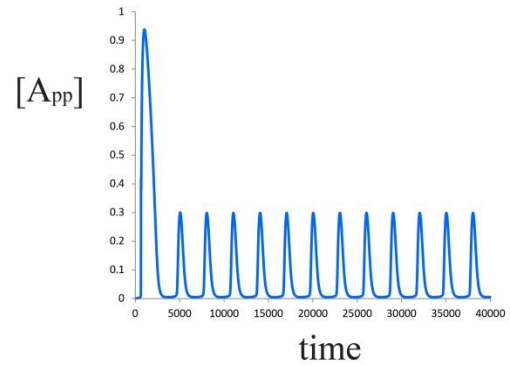
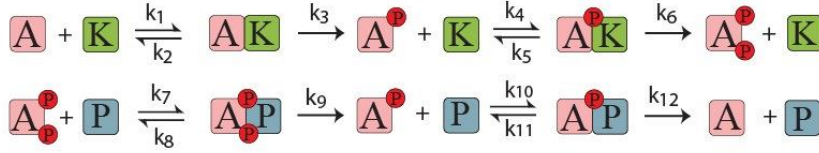


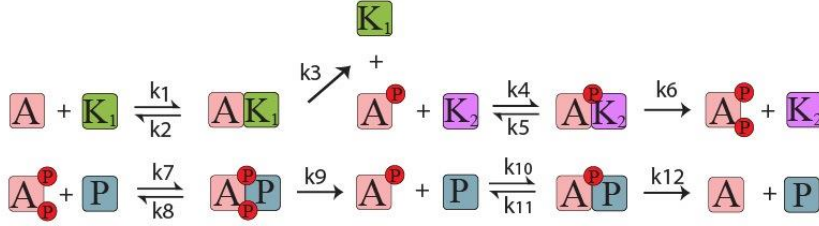
**Figure S5 Effect of downstream coupling to open systems.** (a) shows a schematic diagram of ordered distributive double-site phosphorylation models with downstream coupling to open substrate system of single covalent modification cycle (model R6). (b) shows that model R6 is capable of generating sustained oscillations.



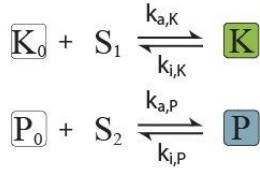
(a) Ordered, double distributive phosphorylation (model M1)



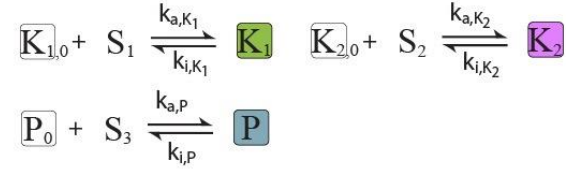
(b) Ordered, double phosphorylation through different kinases (model M2)



(c) Explicit enzymatic activation (for model E1)

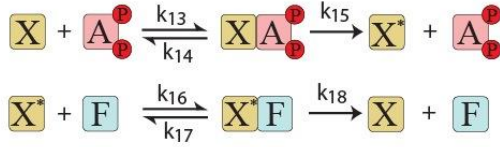


(d) Explicit enzymatic activation (for model E2)

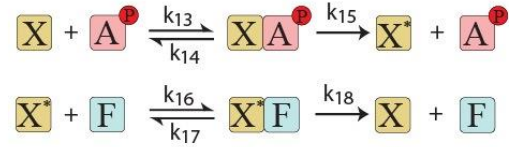


(e) Downstream covalent modification cycle (CMC) in case of downstream coupling

(i) model R1 (and for model R4)



(ii) model R2 (and for model R5)



(iii) model R3

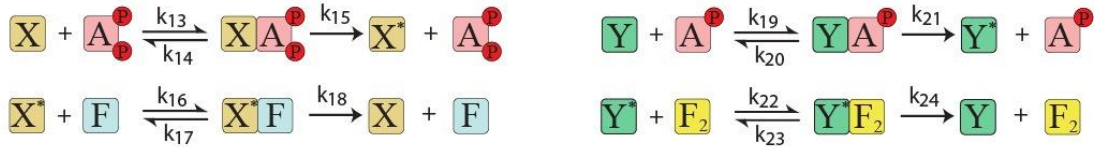


**Figure S6 Depiction of reactions in ordered, double site distributive phosphorylation models with upstream/downstream coupling.** (a) Isolated double-site phosphorylation system with common kinase and phosphatase, model M1. (b) Isolated double-site systems with separate kinases and common phosphatase, model M2. (c) Explicit enzymatic activation, models E1 and E2. Note that the signals  $S_1$ ,  $S_2$ ,  $S_3$  are not consumed: they mediate a simple transition (c,d). (e) Downstream covalent modification cycle: (i) model R1, (ii) model R2 and model R3.

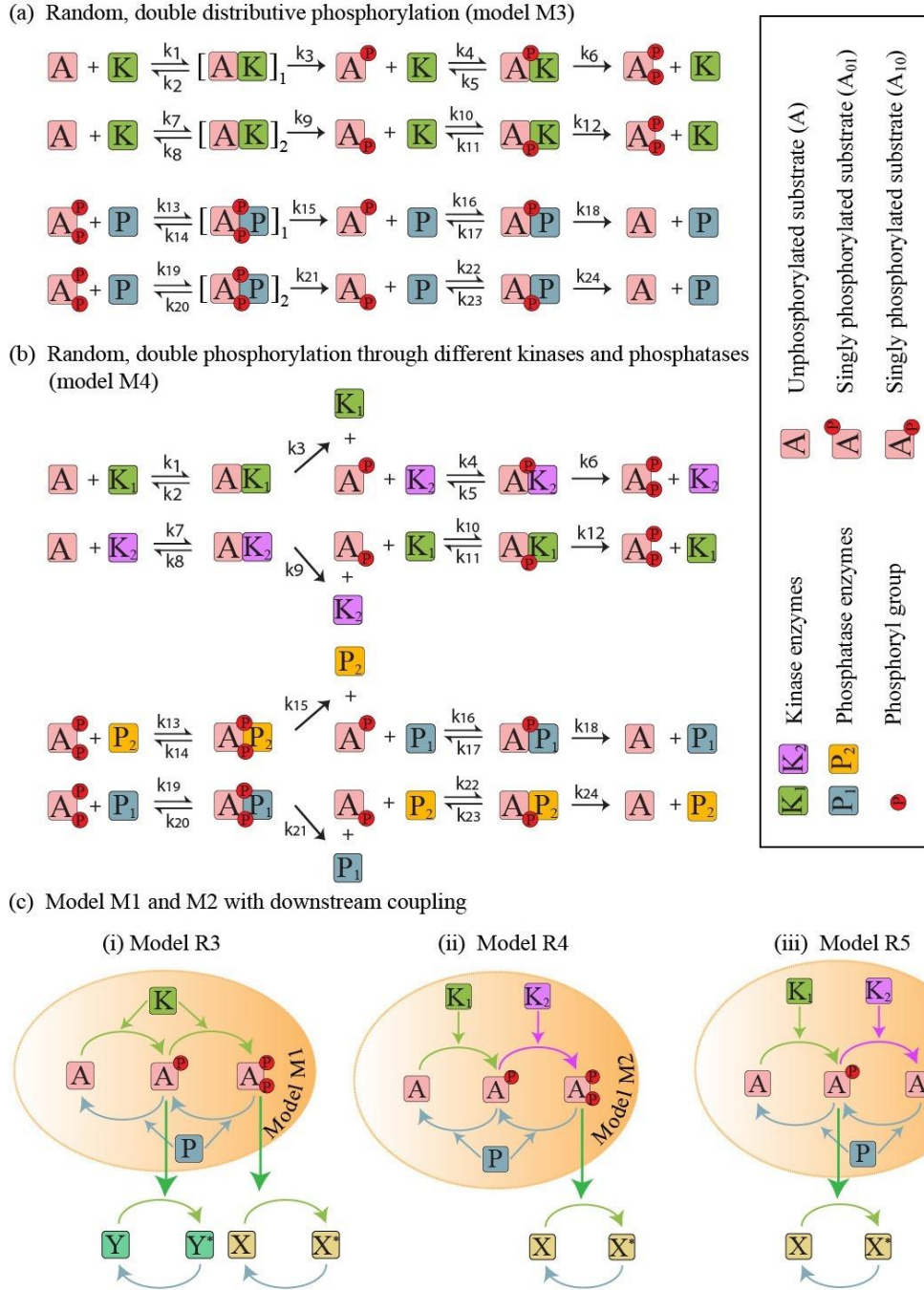


**Figure S7** Reaction depiction of random, double-site distributive phosphorylation models (isolated systems) and ordered, double-site models (model M2) with downstream coupling. (a) Isolated random double-site phosphorylation system with common kinase and phosphatase, model M3. (b) Isolated random double-site systems with separate kinases and separate phosphatases, model M4. (c) Model variants depicting a double site modification model with common/different kinases and common phosphatases, with downstream coupling. Phosphorylation in the downstream covalent modification cycle is catalysed by (i) both modified forms (model R3), (ii) fully modified form (model R4) and (iii) partially modified form (model R5).

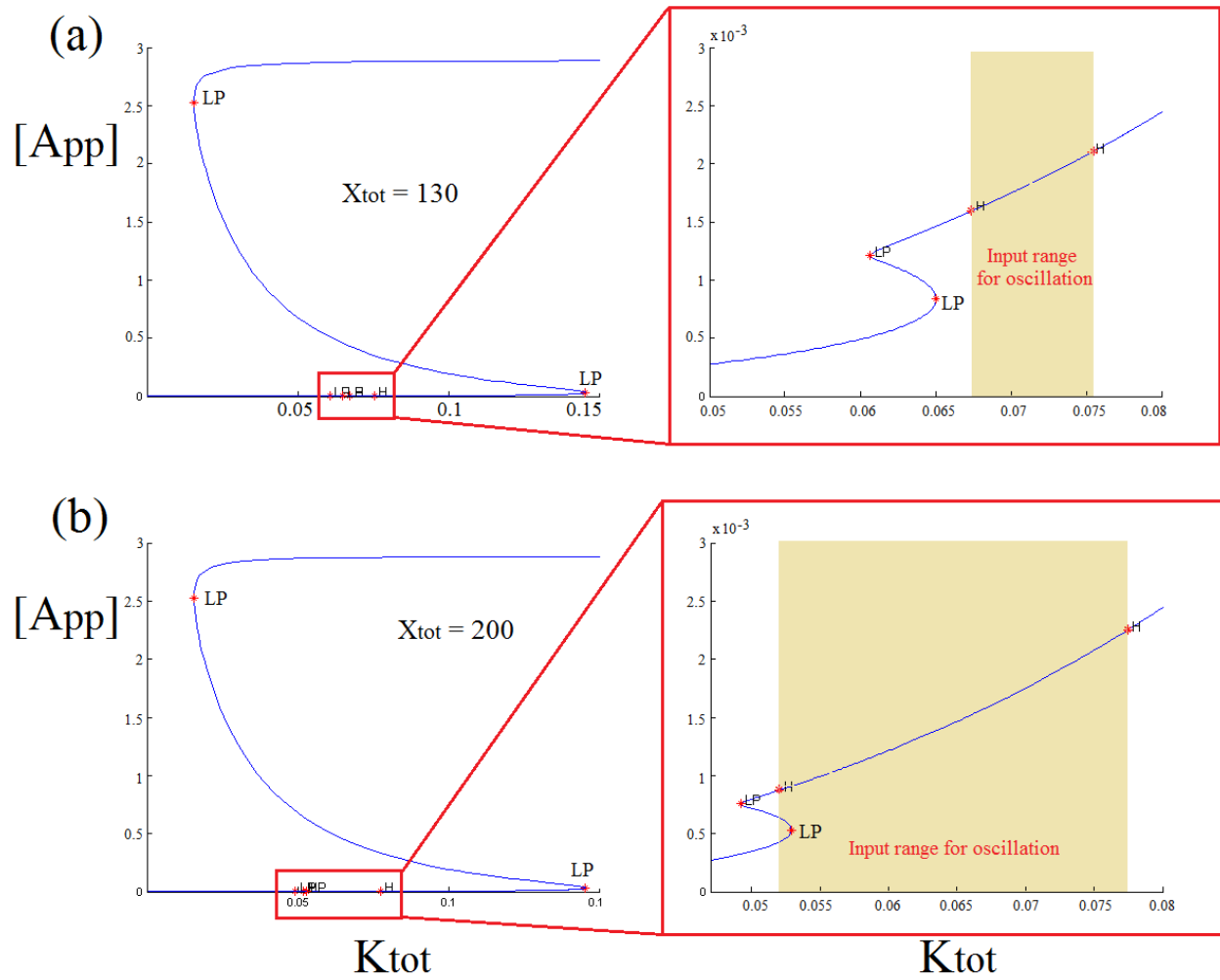


**Figure S8 Effect of downstream coupling on the behaviour of double-site distributive phosphorylation (model R1) in the bistable regime.** (a) shows that while the isolated system is bistable (figure 7a(i) in the main text), downstream coupling introduces tristability, followed by oscillations. (b) shows that increasing the degree of downstream sequestration results in a Hopf bifurcation originating in the regime of tristability